NAWCWPNS TP 8271

SOLID-STATE PHOTODECOMPOSITION OF ENERGETIC NITRAMINES (RDX AND HMX)

by
Clifford D. Bedford and Pamela S. Carpenter
Energetic Materials Branch
Airframe, Ordnance, and Propulsion Division

Melvin P. Nadler
Chemistry and Materials Branch
Research and Technology Division

MAY 1996

NAVAL AIR WARFARE CENTER WEAPONS DIVISION
CHINA LAKE, CA 93555-6001

Approved for public release; distribution is unlimited.

Naval Air Warfare Center Weapons Division

FOREWORD

This report describes a study conducted by the personnel of the Naval Air Warfare Center Weapons Division, China Lake, to investigate the solid-state photodecomposition of the energetic nitramines RDX and HMX using direct sunlight and medium-pressure mercury lamp irradiation. The effort was managed and executed through the Environmental Project Office under the auspices of the Naval Air Systems Command. Funds to support this effort were provided under Work Order N0001994WXC8KDL.

This report was reviewed for technical accuracy by T. AtienzaMoore and R. Quintana.

Approved by
D. GOSS, *Head*
Airframe, Ordnance,
and Propulsion Division
23 May 1996

Under authority of
D. B. McKINNEY
RAdm., U.S. Navy
Commander

Released for publication by
S. HAALAND
Director for Research and Engineering

NAWCWPNS Technical Publication 8271

Published by ..... Scientific and Technical Documentation
Collation ..... Cover, 11 leaves
First printing ..... 100 copies

REPORT DOCUMENTATION PAGE

Form Approved
OMB No. 0704-0188

1. AGENCY USE ONLY (Leave blank)	2. REPORT DATE	3. REPORT TYPE AND DATES COVERED
	May 1996	Summary

4. TITLE AND SUBTITLE

SOLID-STATE DECOMPOSITION OF ENERGETIC NITRAMINES (RDX AND HMX)

5. FUNDING NUMBERS

Work Order N0001994WXC8KDL

6. AUTHOR(S)

Clifford D. Bedford, Pamela S. Carpenter, and Melvin P. Nadler

7. PERFORMING ORGANIZATION NAME(S) AND ADDRESS(ES)

Naval Air Warfare Center Weapons Division
1 Administration Circle
China Lake, CA 93555-6001

8. PERFORMING ORGANIZATION REPORT NUMBER

NAWCWPNS TP 8271

8. SPONSORING/MONITORING AGENCY NAME(S) AND ADDRESS(ES)

Naval Air Systems Command
1421 Jefferson Davis Hwy
Arlington, VA 22243-5120

10. SPONSORING/MONITORING AGENCY REPORT NUMBER

11. SUPPLEMENTARY NOTES

12a. DISTRIBUTION/AVAILABILITY STATEMENT

A statement

12b. DISTRIBUTION CODE

13. ABSTRACT (Maximum 200 words)

(U) A study was undertaken to investigate the solid-state photodecomposition of the energetic nitramines RDX and HMX using direct sunlight and medium-pressure mercury lamp irradiation. The rate of RDX photolysis is faster than the rate of HMX photolysis at high concentrations (>2 wt%) and about the same for concentrations below 2 wt%. Both RDX and HMX photodecompose in KBr at an exponential rate that depends on concentration, path length, wavelength, and intensity of light. Moreover, preliminary data show that the rate may be also dependent on particle size. The only solid products characterized in the photodecomposition reactions were the inorganic salts potassium nitrate (KNO_3) and potassium nitrite (KNO_2), and the organic formamides such as methyl formamide and formamide. The desert environment offers a unique opportunity to exploit solar energy in an effort to reclaim explosive-contaminated lands and to remediate chemically-contaminated sludge. The preliminary results reported in this publication indicate that solid-state photodecomposition of energetic nitramines is a potentially cost effective and efficient method for remediating contaminated desert environments.

14. SUBJECT TERMS

Photodecomposition, Nitramines, RDX, HMX, Lamp Irradiation, Photolysis

15. NUMBER OF PAGES

20

16. PRICE CODE

17. SECURITY CLASSIFICATION OF REPORT	18. SECURITY CLASSIFICATION OF THIS PAGE	19. SECURITY CLASSIFICATION OF ABSTRACT	20. LIMITATION OF ABSTRACT
UNCLASSIFIED	UNCLASSIFIED	UNCLASSIFIED	SAR

CONTENTS

INTRODUCTION AND BACKGROUND

As part of a Department of Defense global program, the Navy has initiated efforts to develop benign, cost effective, environmentally friendly processes for the remediation of facilities contaminated with hazardous energetic materials. One process particularly appropriate for the Naval Air Warfare Center Weapons Division, China Lake, California, is the exploitation of photochemical degradation for the decomposition of the ubiquitous energetic nitramines cyclotrimethylenetrinitramine (RDX) and cyclotetramethylenetetranitramine (HMX) used in research and development programs involving numerous ordnance items.

Research, development, and production facilities for nitramine-containing explosives and propellant systems have inevitably resulted in areas contaminated with nitramine residue. These areas must be cleaned and decontaminated before a change in their use can be undertaken. Because it is Navy policy to manage its land holdings in a clean, safe, and environmentally friendly manner, a program was undertaken to determine the effectiveness and efficiency of photodecomposing nitramine-contaminated soil.

The effort was based on the assumption that the high-intensity solar irradiation available to government installations in the Southwestern United States could provide an economic and effective way to destroy these unwanted contaminants. It was further assumed that the process would afford benign photochemical decomposition by-products that would not adversely impact the fragile desert environment.

The photochemical decomposition of nitramine compounds has been examined by a number of researchers (References 1-5). All of these investigations were carried out in aqueous solutions. The addition of catalysts or rate accelerators was also explored. The principal objective of these earlier studies centered on the development of an aqueous process for the remediation of nitramine-contaminated lagoons and/or waste streams. Although both catalyzed and uncatalyzed processes were completely effective, the concentration of dissolved nitramine in the water (approximately 100 ppm for RDX and 10 ppm for HMX) precluded these methods from being commercially attractive. On the other hand, the potential for the solid-state photodecomposition of nitramines has not been explored. Examination of the literature revealed that only low-temperature, high-energy irradiation of the nitramines has been studied. The lack of available literature data, coupled with the potential for economic, effective, and efficient remediation of large nitramine-contaminated areas, were excellent drivers for the current investigation.

Before embarking on a demonstration program directed toward defining the efficiency of a solar photochemical decomposition effort for energetic nitramines, two fundamental technology questions must be answered. First, is the solid-state photochemical decomposition rate for RDX and HMX by direct sunlight sufficiently robust to afford an efficient process? Second, are the final photodecomposition products of these energetic nitramines environmentally benign? Our preliminary findings, which are detailed in this report, clearly indicated that both energetic nitramines (RDX and HMX) are effectively and efficiently destroyed in the solid state by either a medium-pressure mercury (Hg) lamp ultraviolet light source or solar irradiation, and that the residual photolysis by-products do not appear to be a major concern. The study reported herein defines the photolysis conditions used and the results obtained for the

solid-state photodecomposition of energetic nitramines (RDX and HMX). In addition, we have indicated areas that require additional investigation before we can develop an appropriate test protocol for photochemical remediation of nitramine-contaminated sites.

RESULTS AND DISCUSSION

FTIR CALIBRATION OF THE WEIGHT PERCENT OF RDX AND HMX

The first program objective was to establish a Fourier transform infrared (FTIR) method to measure the weight percent of RDX and HMX in a transparent matrix to quantitatively monitor their photochemical degradation. To accomplish this task, a series of potassium bromide (KBr) pellets containing between 0.5 to 5% nitramine in a total weight of 150.0 ±0.5 mg were prepared. The pellets were pressed under vacuum at 40,000 psi for 2 minutes affording clear, colorless glasses of constant thickness or path length. These pellets were then scanned using a Nicolet 710 FTIR spectrometer at 4 cm^{-1} resolution with a deuterated triglycine sulfate (DTGS) uncooled detector and a 450 cm^{-1} cut-off.

Initially, the absorption region between 3050 and 2950 cm^{-1} was used to measure the decomposition rates. However, after prolonged medium-pressure Hg lamp or solar exposure, scattering decreased the transmittance in this region to less than 5%. To overcome the effect of high-frequency scattering, we used weak bands in the low frequency region (590 and 754 cm^{-1} for RDX and 658 and 830 cm^{-1} for HMX). Figures 1-3 show plots of the peak heights at the above frequencies with the baseline limits shown in parentheses versus the wt% of nitramine. The HMX data are fit to a straight line for the 2.5-5.5 wt% region (Figure 1) and to a second-order polynomial for the 0-2.5 wt% region (Figure 2). Based on spectral clarity and isolation, the 658 cm^{-1} peak is used for HMX. The equations for determining the HMX wt% are as follows:

$$\text{HMX (wt\%)} = 4.355(\text{p658}) - 0.248 \quad \text{for 2.5 - 5.5 wt\%} \tag{1}$$

$$\text{HMX (wt\%)} = 4.55(\text{p658})^2 + 1.334(\text{p658}) - 0.0056 \quad \text{for 0 - 2.5 wt\%} \tag{2}$$

where p658 is the peak height at 658 cm^{-1} with baseline limits of 677-640 cm^{-1}. The linear correlation coefficient (R^2) value of 0.9669 for both fits is reasonable, considering the non-Beers Law behavior of the data. Figure 3 shows the calibration curves for the RDX data which are fit to a second-order polynomial for the entire 0-5 wt% range. The 590 cm^{-1} RDX peak is used to determine the RDX wt% and the equation is shown below.

$$\text{RDX (wt\%)} = 1.824(\text{p590})^2 + 1.848(\text{p590}) + 0.0521 \tag{3}$$

where p590 is the peak height at 590 cm^{-1} with baseline limits of 640-530 cm^{-1}. The R^2 value is 0.9858 for the curve fit.

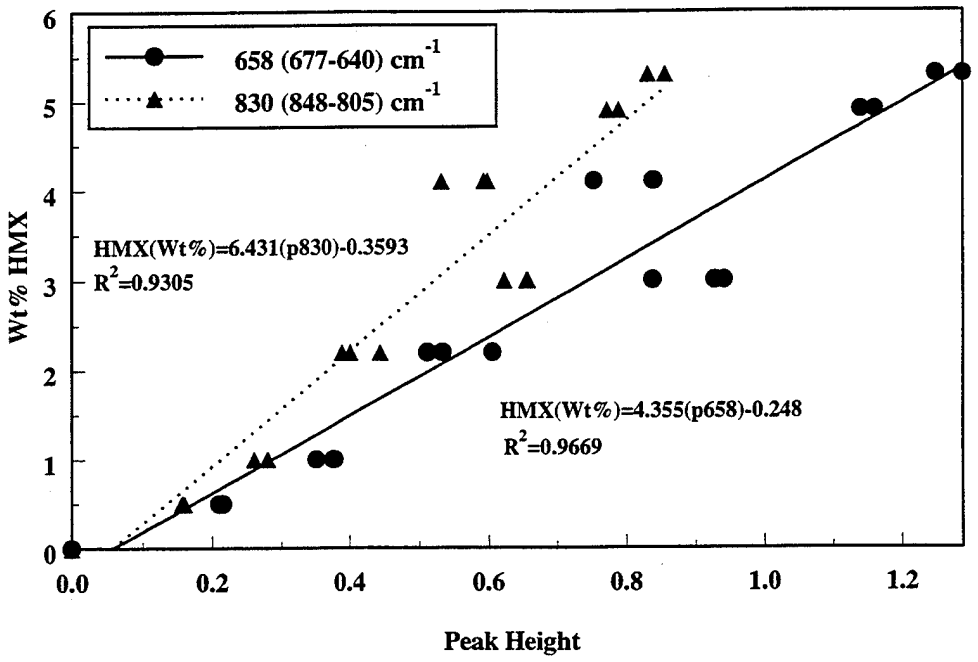

FIGURE 1. HMX FTIR Calibration (2.5 - 5.5 wt%).

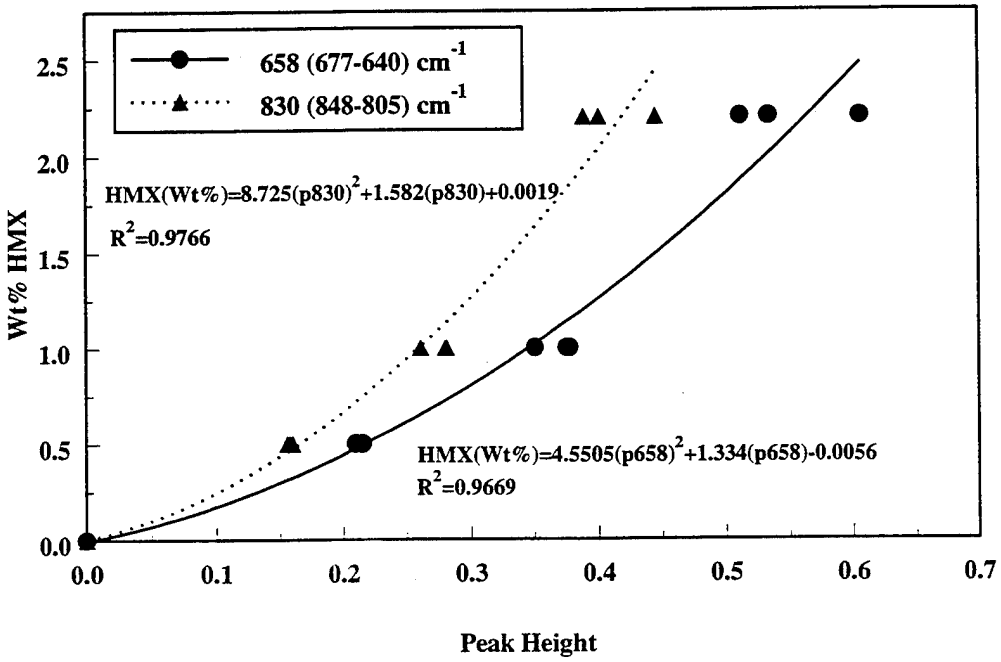

FIGURE 2. HMX FTIR Calibration (0 - 2.5 wt%).

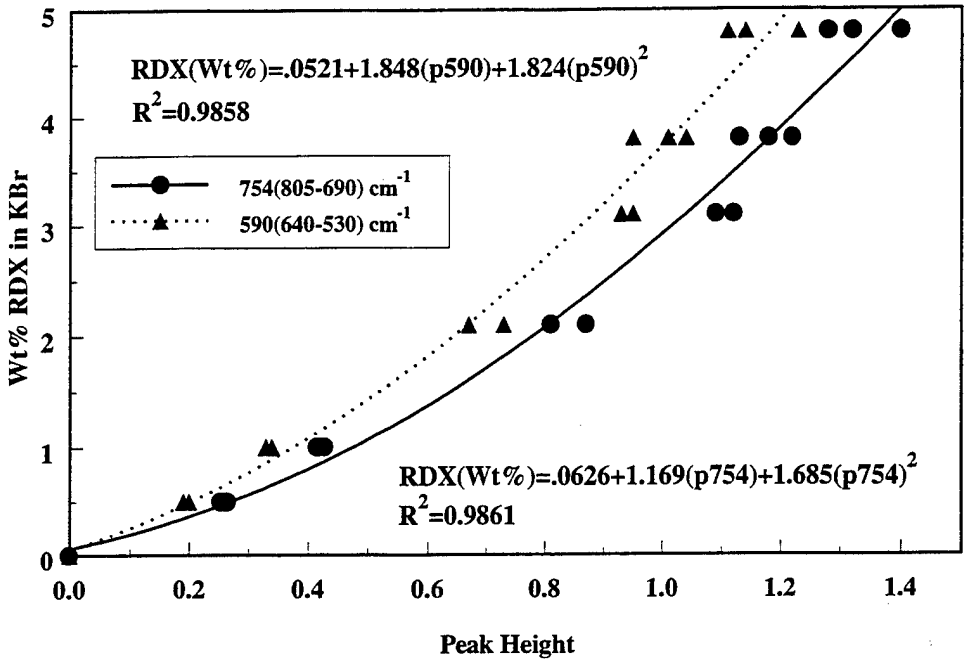

FIGURE 3. RDX FTIR Calibration (0 - 5 wt%).

Hg LAMP IRRADIATION OF RDX AND HMX SUSPENDED IN KBr PELLETS

Two sets of RDX and HMX pellets (described above) with concentrations varying between 0.5 and 5.0 wt% nitramine were exposed to an unfiltered medium-pressure Hg lamp. The disappearance of the RDX and HMX was monitored as a function of time using the FTIR wt% calibrations just discussed. An exponential decay rate expression (Equation 4) gives an excellent fit to most of the photodecomposition data. However, at high HMX wt% (> 3 wt%), the decay is almost linear.

$$\text{wt\% (nitramine)} = a\, e^{-(bt)} \qquad (4)$$

The pre-exponential factor "a" is the wt% intercept (t = 0), where "t" is the irradiation time in hours and "b" is the exponential slope. The exponential rate expression does not indicate an overall mechanism but is used to compare all the data on an equal basis using the exponential slopes and the wt% intercepts. In general, excellent agreement was observed for the duplicate samples. Representative examples of RDX and HMX Hg lamp photodecompositions at 1 and 5 wt% are shown in Figures 4 and 5, respectively. Table 1 lists the measured concentration in wt%, the wt% intercept, the exponential slope, and the calculated half-life for all the RDX and HMX samples exposed to the Hg lamp. A plot of the exponential photolysis rates (b) versus the wt% intercepts (a) for both RDX and HMX is shown in Figure 6. The RDX and HMX photodecomposition rate is faster at lower wt% or concentration, but the rate decreases and starts to "level off" at higher wt% (Table 1 and Figure 6). Moreover, the photodecomposition rate of RDX is significantly faster than that of HMX at higher concentrations, but the rates are closer at low wt%. Figure 7 shows a plot of the exponential half-life in hours versus the wt% intercept for all the RDX and

HMX samples exposed to the Hg lamp. The half-life data show that, for the initial half of the photolysis, both RDX and HMX have about the same half-life at low wt% (0.5-1.0 wt%), but, as the wt% increases, HMX takes progressively longer to photodecompose than RDX (Figure 7). It is clear that the Hg lamp photodecomposition rate of both RDX and HMX in KBr pellets increases with decreasing concentration or, more exactly, optical density (optical density = concentration × path length). Since the KBr pellets were made under the same experimental conditions and have the same total weight of KBr, their thickness or path length is nearly constant. The constant path length is confirmed from the good fit of the calibration data in Figures 1-3.

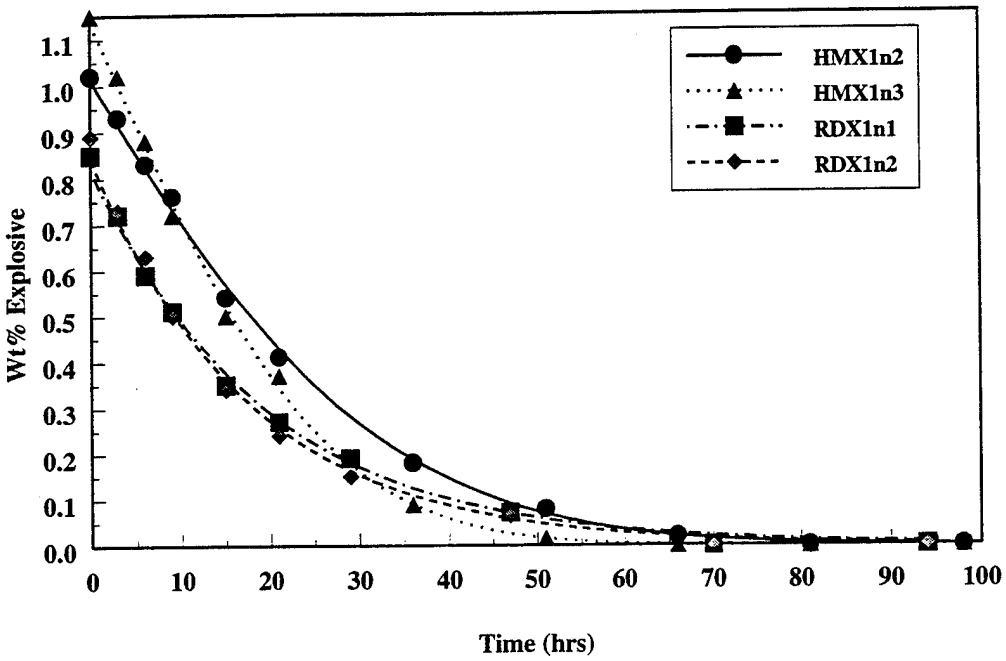

FIGURE 4. Comparison of HMX and RDX Photolysis with Hg Lamp (1 wt%).

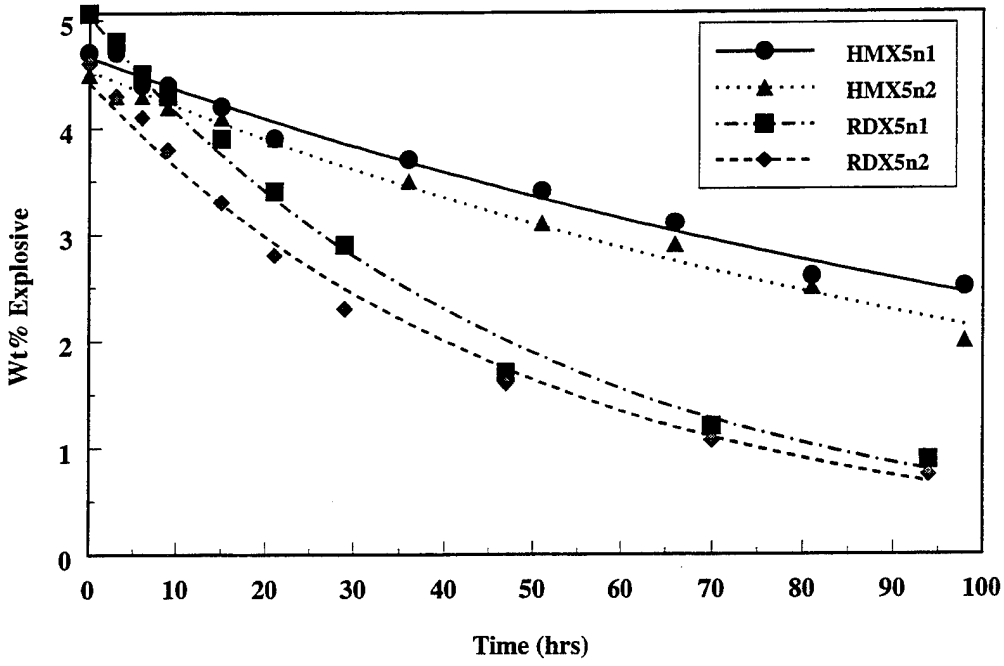

FIGURE 5. Comparison of HMX and RDX Photolysis with Hg Lamp (5 wt%).

TABLE 1. Medium-Pressure Hg Lamp Photochemical Decomposition Rate Expression for Various RDX and HMX Concentrations.

RDX Sample #	Nominal [RDX], %	Exponential "a" Term	Exponential "b" Term	R^2	Half-life, hrs
2	0.5	0.49	0.081	0.9958	8.6
3	0.5	0.47	0.079	0.9960	8.8
4	1.0	0.89	0.062	0.9989	11.2
5	1.0	0.84	0.055	0.9982	12.6
6	2.0	2.09	0.036	0.9987	19.5
7	2.0	2.35	0.037	0.9993	18.7
8	3.1	3.54	0.035	0.9994	20.0
9	3.8	3.71	0.027	0.9973	25.6
10	3.8	3.61	0.032	0.9967	22.0
11	4.8	5.03	0.020	0.9941	34.7
12	4.8	4.43	0.020	0.9936	34.7

TABLE 1. (Continued).

HMX Sample #	Nominal [HMX], %	Exponential "a" Term	Exponential "b" Term	R^2	Half-life, hrs
2	0.5	0.52	0.061	0.9982	11.4
3	0.5	0.49	0.090	0.9881	7.7
4	1.0	1.07	0.046	0.9948	15.1
5	1.0	1.20	0.058	0.9947	12.0
6	2.2	2.63	0.019	0.9703	37.3
7	2.2	1.99	0.025	0.9866	28.1
8	3.0	3.34	0.016	0.9699	44.7
9	3.0	4.06	0.014	0.9874	51.3
10	4.1	3.62	0.008	0.9458	82.5
11	4.9	4.66	0.007	0.9867	105.0
12	5.3	4.54	0.008	0.9892	90.0

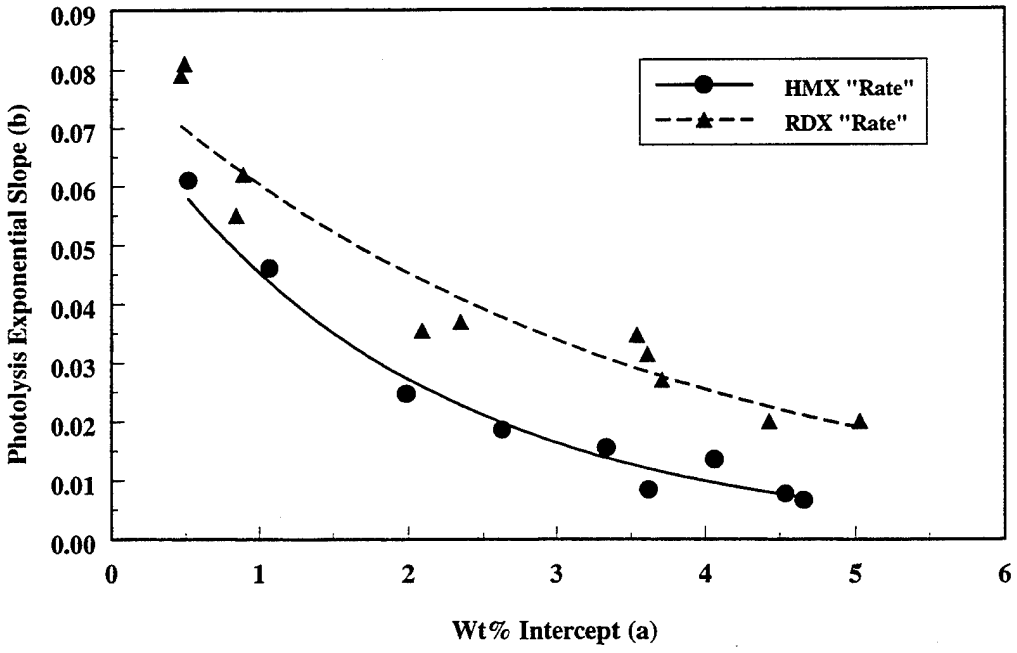

FIGURE 6. Comparison of HMX and RDX Exponential Rates for Hg Lamp Irradiation.

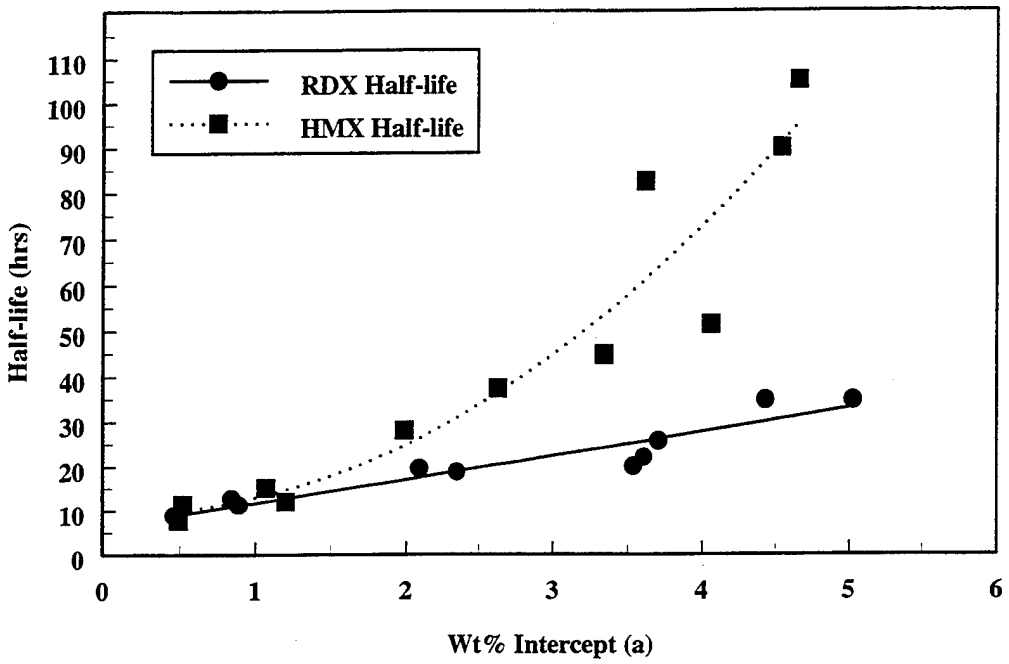

FIGURE 7. Comparison of HMX and RDX Half-lives for Hg Lamp Irradiation.

SOLAR IRRADIATION OF RDX AND HMX IN KBr PELLETS

Another set of RDX and HMX pellets (prepared as described above) at the same concentrations was exposed to quartz-filtered solar irradiation. Representative examples of RDX and HMX solar photodecompositions at 1 and 5 wt% are shown in Figures 8 and 9, respectively. Again, both RDX and HMX samples degraded with time. However, the rate of photochemical degradation is significantly slower for the solar-irradiated materials as compared to the Hg-lamp-irradiated samples. Whereas the duration for the Hg lamp experiments was measured in hours, the duration of the solar experiments was measured in weeks. The disappearance of nitramine was again fit to an exponential decay equation (Equation 4). Table 2 lists the measured concentration of RDX and HMX, the wt% intercept, the exponential slope, and the calculated half-life (in weeks) at each concentration. The RDX solar photodecomposition rate is faster than that observed for HMX at the higher concentrations, but about equal at the lower concentrations (Table 2). As in the Hg lamp photolysis, the sun-irradiated explosive decomposition rate increased at the lower concentrations or lower optical densities. Figure 10 is a plot of the half-life for sun-irradiated RDX and HMX versus the wt% intercept (data from Table 2). Note the similarity between Figure 7 (Hg lamp irradiation) and Figure 10 (sun irradiation), except for the much longer half-lives for sun irradiation.

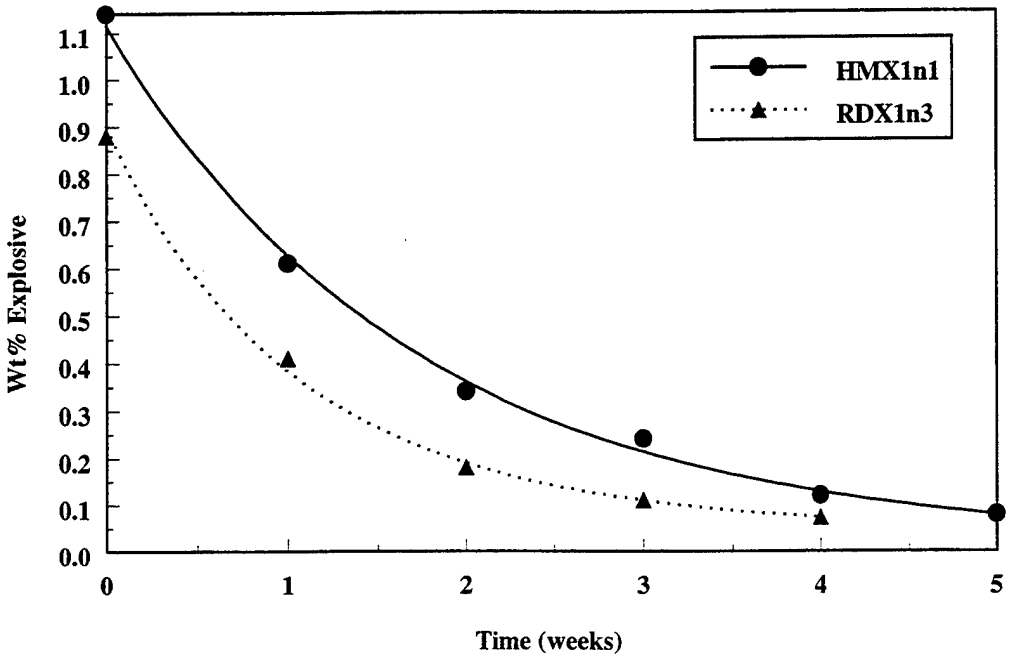

FIGURE 8. Comparison of HMX and RDX Photolysis with Sun Irradiation (1 wt%).

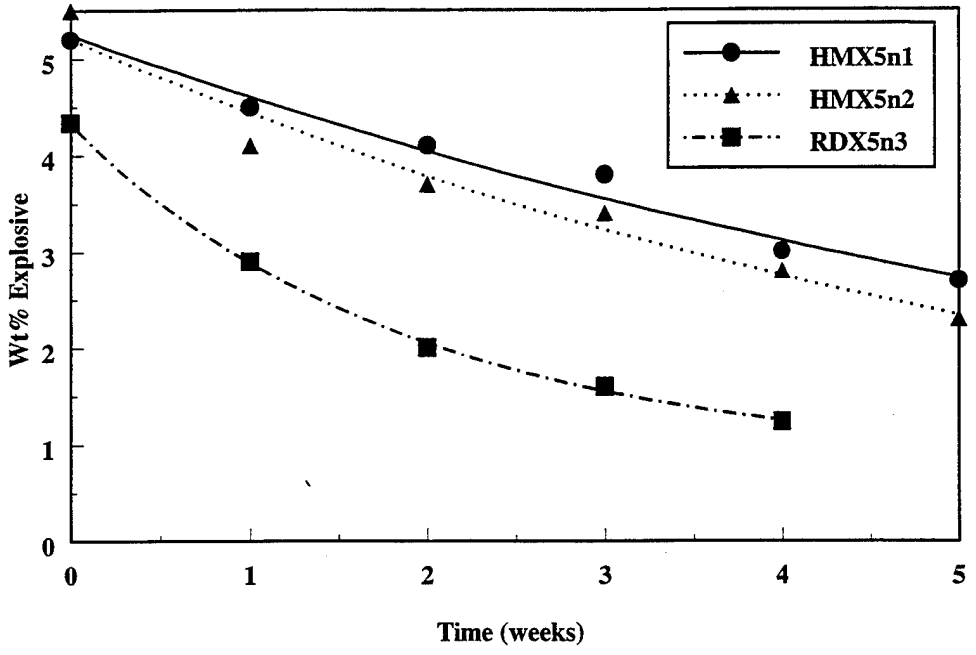

FIGURE 9. Comparison of HMX and RDX Photolysis with Sun Irradiation (5 wt%).

TABLE 2. Solar Photochemical Decomposition Rate Expressions for Various RDX and HMX Concentrations.

RDX Sample #	Nominal [RDX], %	Exponential "a" Term	Exponential "b" Term	R^2	Half-life, wks
1	0.5	0.48	0.615	0.9721	1.10
2	1.0	0.88	0.740	0.9966	0.93
3	2.0	2.08	0.459	0.9917	1.50
4	3.1	3.30	0.427	0.9942	1.60
5	3.8	3.88	0.384	0.9840	1.80
6	4.8	4.25	0.341	0.9880	2.00
HMX Sample #	**Nominal [HMX], %**	**Exponential "a" Term**	**Exponential "b" Term**	**R^2**	**Half-life, wks**
1	0.5	0.50	0.657	0.9981	1.0
2	1.0	1.13	0.571	0.9964	1.2
3	2.0	1.89	0.320	0.9816	2.2
4	3.0	3.89	0.216	0.9647	3.2
5	4.1	3.53	0.180	0.9520	3.8
6	4.9	5.26	0.164	0.9619	4.2
7	5.3	5.21	0.127	0.9790	5.5

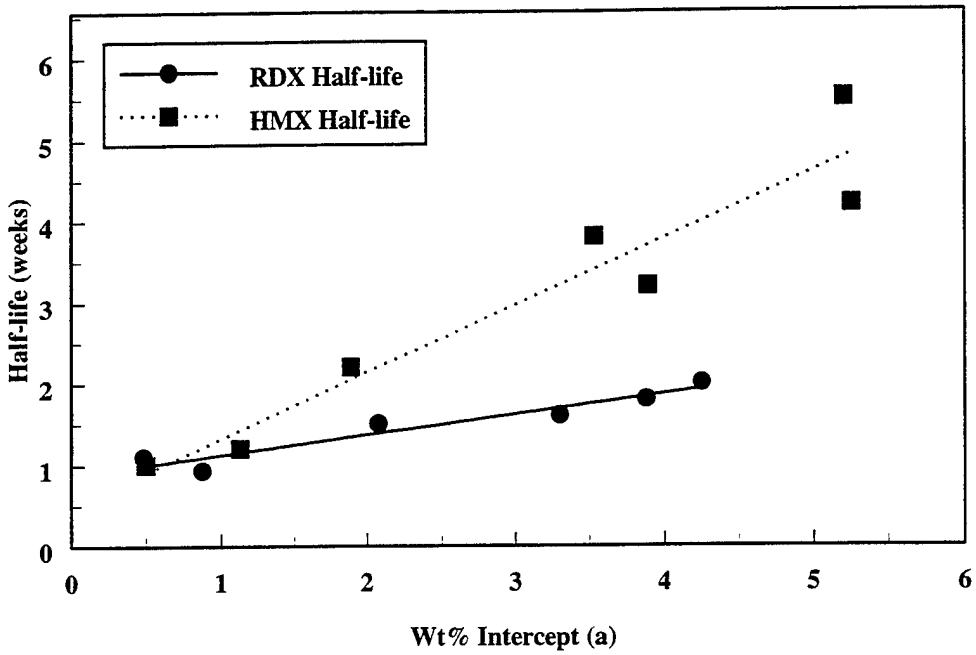

FIGURE 10. Comparison of HMX and RDX Half-lives for Sun Irradiation.

Although numerous differences existed between the Hg lamp and solar photodecomposition experiments (such as humidity, length of exposure, filter, intensity of light, and temperature), the relative rate behavior for HMX and RDX decomposition appeared quite consistent. Figures 11 and 12 show comparisons of HMX and RDX at 1 wt% for Hg lamp versus solar photodecomposition with the solar exposure time-scale converted to actual hours of irradiation. The slower photolysis rate for sun irradiation compared to Hg lamp irradiation indicates a lower intensity of light in the region of HMX and RDX absorption (below about 300 nm). However, given enough time, even HMX at 5 wt% will completely photodecompose under sun irradiation.

A series of uncalibrated KBr pellets containing RDX and HMX was prepared and exposed for ten weeks to sun irradiation. For this series, the pellet sample size ranged from 400 to 600 mg of KBr containing from 1.0 to 5.0% nitramine. The pellets were pressed at 40,000 psi for one minute. No vacuum was used during pressing operations. These pellets were then scanned with a Digilab FTIR spectrometer at 4 cm^{-1} resolution using a DTGS detector. The resulting pellets had variable path lengths, and peak heights were not calibrated to wt% of explosive. These pellets were used to obtain relative rate data by monitoring the absorbances at the same frequencies used for the calibrated KBr pellets (658 cm^{-1} for HMX and 590 cm^{-1} for RDX) versus sun exposure time in weeks, and then fitting the data to the exponential decay equation (Equation 4). Table 3 lists the measured initial concentration in wt%, the absorbance intercept (a), the exponential slope (b), the half-life in weeks, and the ratio of the calibrated exponential "b" term (Table 2) to the corresponding uncalibrated "b" term (at about the same wt%) for all the uncalibrated HMX and RDX sun-exposed samples. The RDX exponential rates show the decrease in rate with increase in concentration (Table 3) observed for the calibrated constant path length data (Table 2), but the HMX data are inconsistent (Table 3) due to the change in path length. Figures 13-16 show selected plots of the calibrated and uncalibrated sun-irradiated photolysis of HMX and RDX, where the initial uncalibrated absorbance is matched with the initial wt% of the calibrated data. The 4 wt% HMX example in Figure 13 shows an excellent match of the photolysis rates for the first 5 weeks, and indeed the ratio of the calibrated-to-uncalibrated rate (b(calibrated)/b(uncalibrated)) is 0.96 (Table 3). Figure 14 shows the HMX 5 wt% case where the calibrated rate is faster than the uncalibrated rate and b(calibrated)/b(uncalibrated) is 1.7 (Table 3). Figures 15 and 16 show examples for RDX sun-irradiated photolysis where the rates match for 2 wt% [b(calibrated)/b(uncalibrated) = 1.1, Table 3 and Figure 15] and is much faster for 5 wt% [b(calibrated)/b(uncalibrated) = 2.4, Table 3 and Figure 16]. The calibrated and uncalibrated KBr pellets were sun irradiated under identical conditions; therefore, for the samples of equal concentration, the difference in rates must be due to a change in path length or inefficient photolysis of large nitramine particles that did not dissolve in the KBr.

EFFECT OF FILTERS ON THE DECOMPOSITION RATES FOR RDX AND HMX KBr PELLETS

In another set of experiments, a series of uncalibrated KBr pellets containing 1.0% nitramine were exposed to directed sun irradiation. The samples were placed under quartz, Plexiglas, and glass to determine the effect of wavelength on the rates of nitramine degradation. As shown in Figures 17 and 18 for RDX and HMX, respectively, the photodecomposition rates decrease as the intensity in the lower wavelength region (RDX and HMX absorb below about 300 nm) is decreased. Thus, a quartz filter (which allows transmission of wavelengths down to about 200 nm) was significantly better than glass, which, in turn, was better than Plexiglas. Clearly no external filters should be used to ensure effective and efficient decomposition of RDX and HMX. The use of unfiltered, natural sunlight to effectively and efficiently

decompose these ubiquitous energetic nitramines is the most cost effective and environmentally benign method available to the explosive community and should require only a modest facility investment.

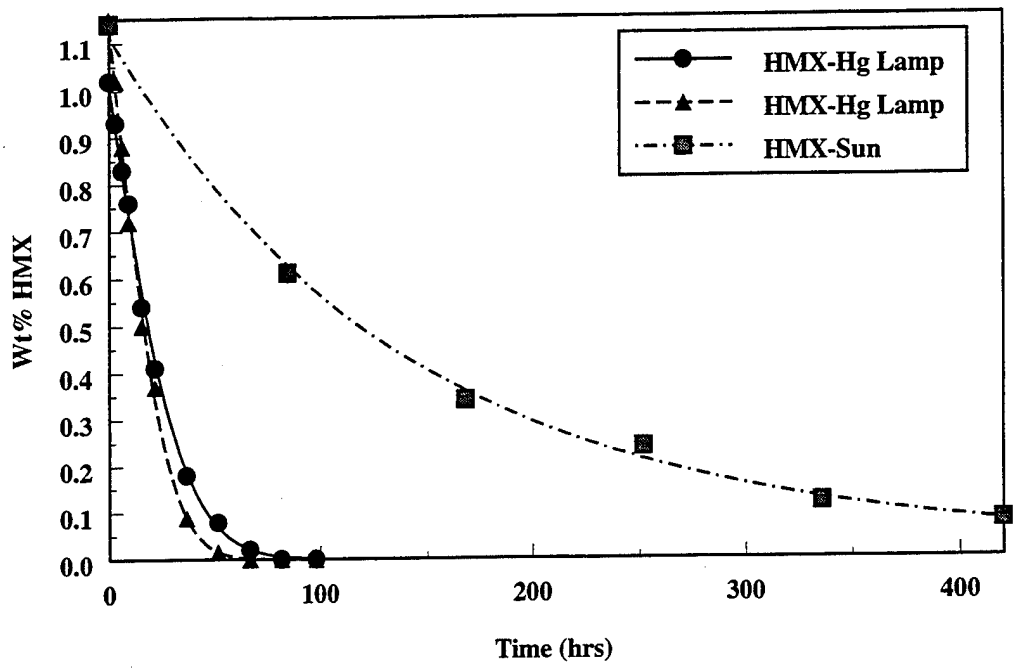

FIGURE 11. Comparison of Hg Lamp and Sun Irradiation for HMX in KBr (1 wt%).

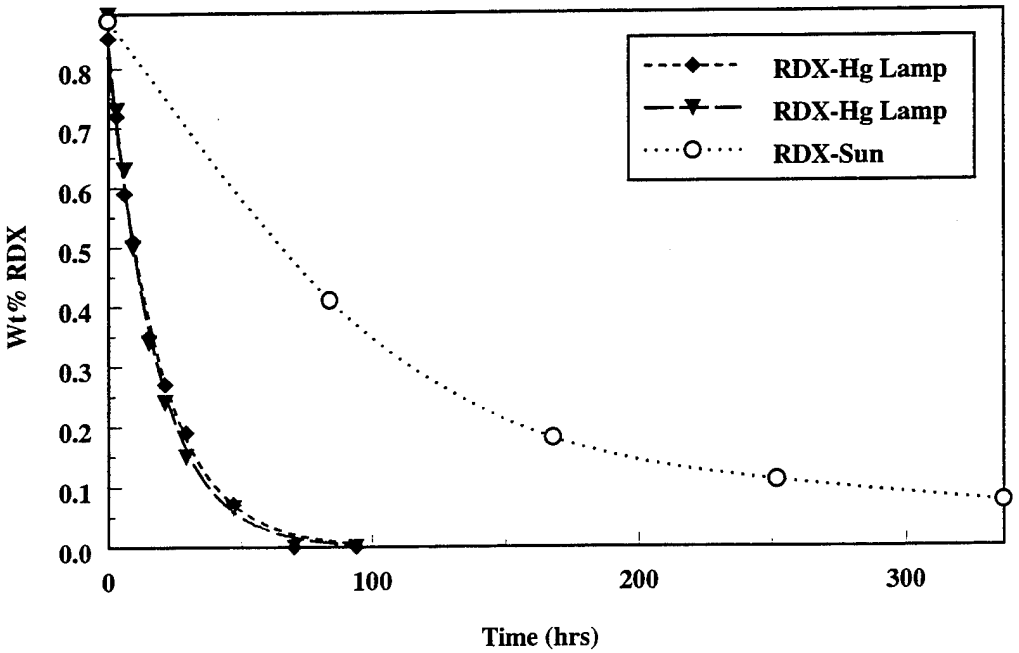

FIGURE 12. Comparison of Hg Lamp and Sun Irradiation for RDX in KBr (1 wt%).

TABLE 3. Solar Photochemical Decomposition Rate Data For Uncalibrated RDX and HMX Samples.

Measured RDX wt%	Exponential "a" Term	Exponential "b" Term	Half-life, wks	Calibrated RDX (b) / Uncalibrated RDX (b)
1	0.25	0.44	1.6	1.70
2	0.50	0.41	1.7	1.10
3	0.48	0.29	2.4	1.50
4	0.69	0.22	3.2	1.70
5	0.82	0.14	5.0	2.40
Measured HMX wt%	**Exponential "a" Term**	**Exponential "b" Term**	**Half-life, wks**	**Calibrated HMX (b) / Uncalibrated HMX (b)**
1	0.29	0.11	6.3	5.20
2	0.60	0.18	3.9	1.80
3	0.76	0.15	4.6	1.30
4	0.97	0.23	3.0	0.96
5	1.43	0.08	8.4	1.70

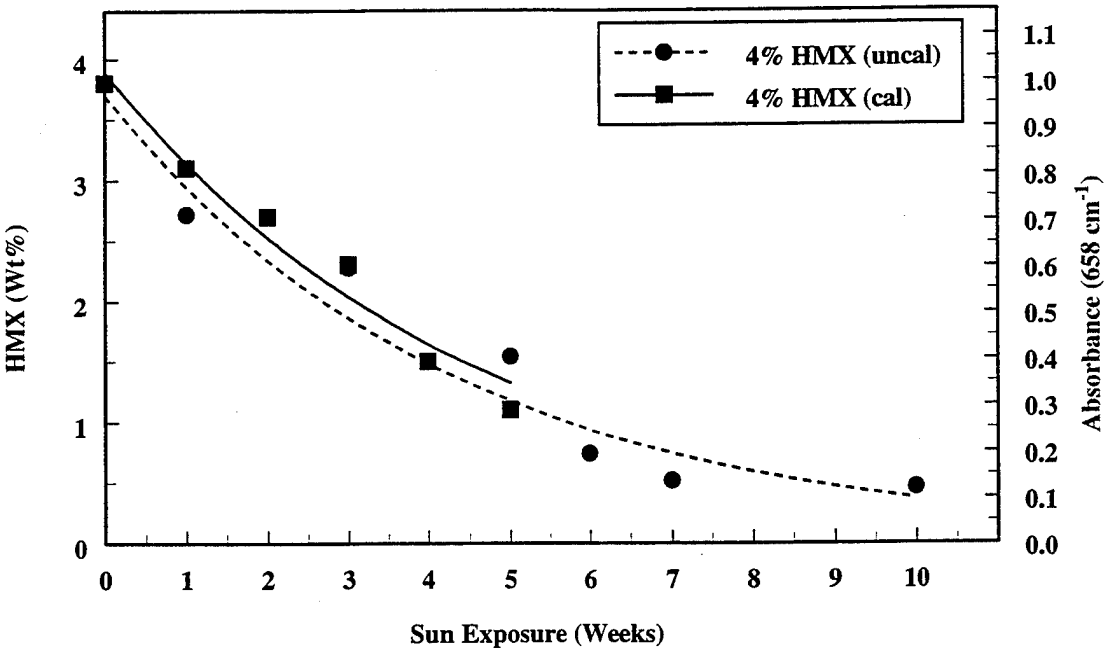

FIGURE 13. Calibrated vs. Uncalibrated HMX Sun Exposure (4 wt%).

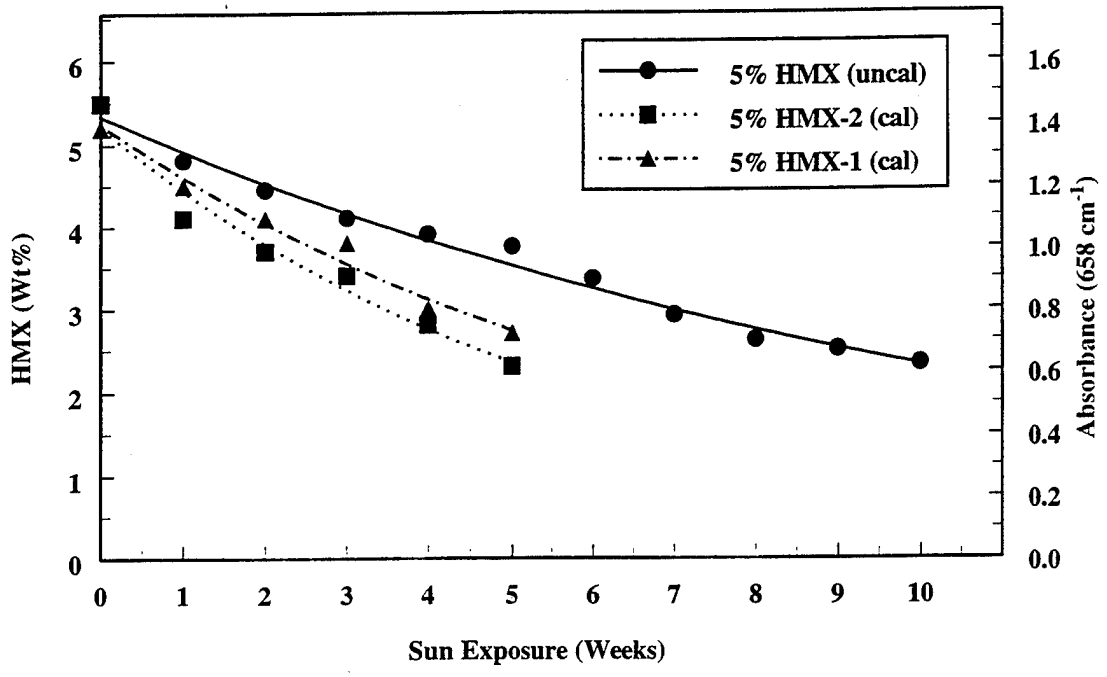

FIGURE 14. Calibrated vs. Uncalibrated HMX Solar Exposure (5 wt%).

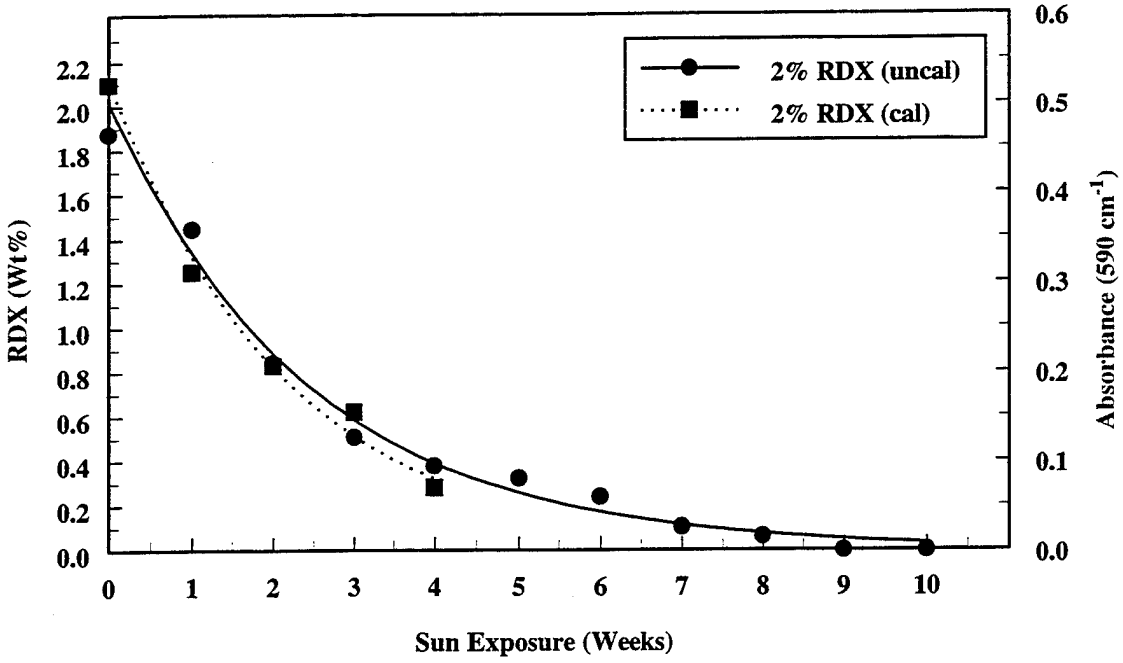

FIGURE 15. Calibrated vs. Uncalibrated RDX Solar Exposure (2 wt%).

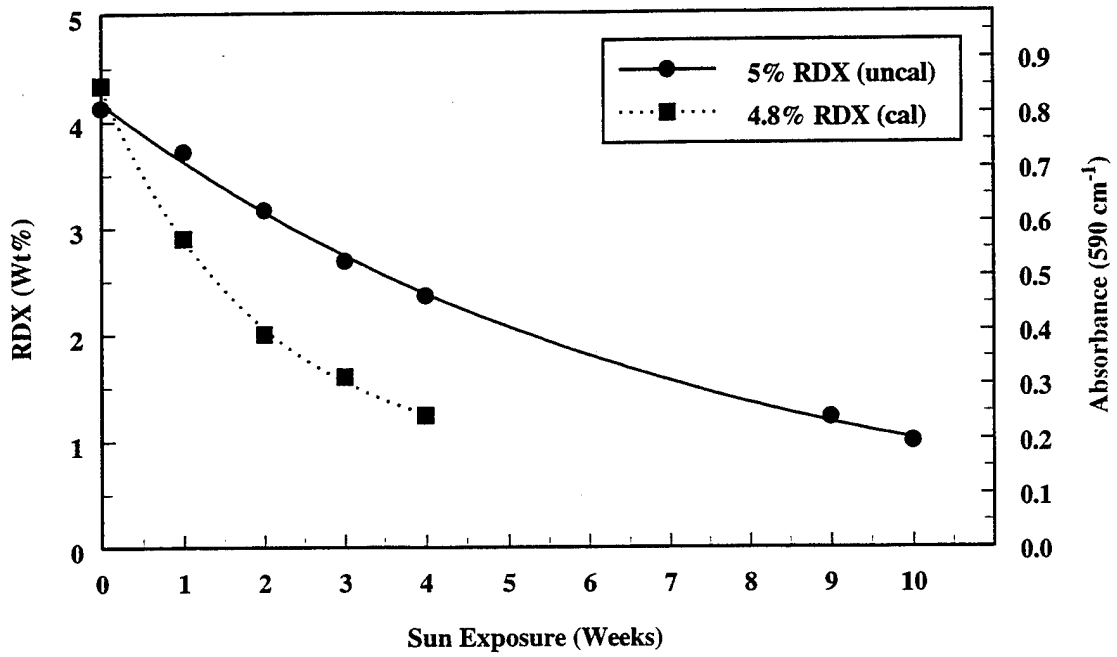

FIGURE 16. Calibrated vs. Uncalibrated RDX Solar Exposure (5 wt%).

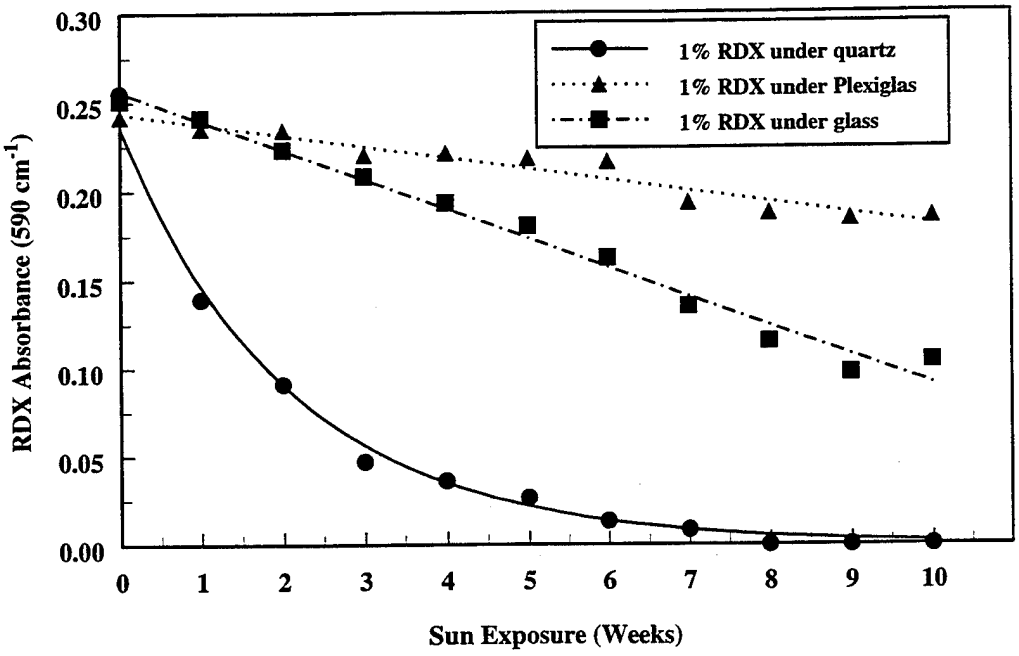

FIGURE 17. Uncalibrated RDX Solar Exposure Under Wavelength Filters (1 wt%).

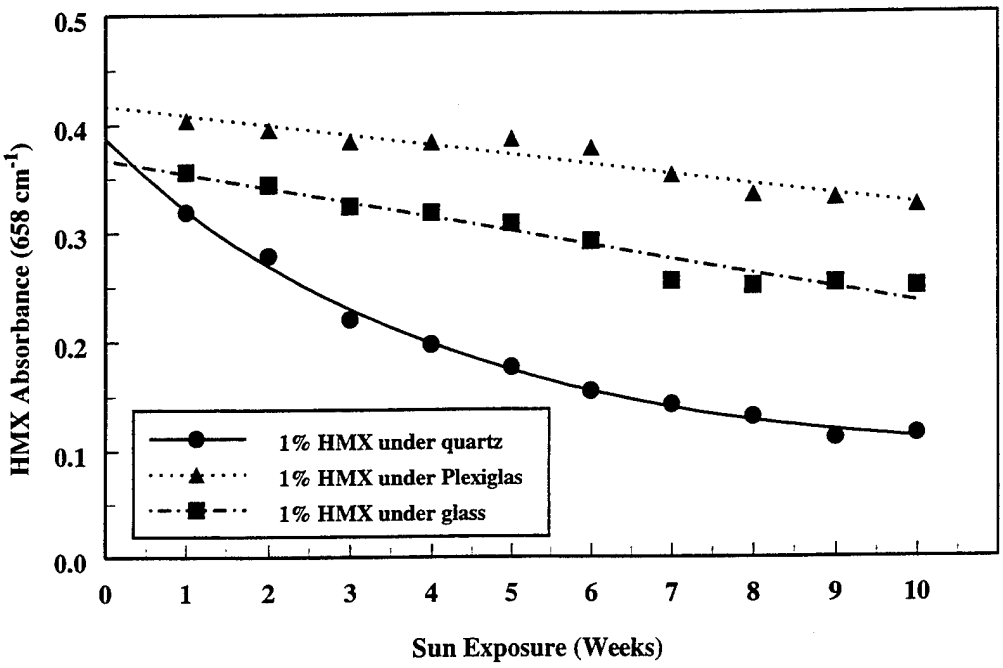

FIGURE 18. Uncalibrated HMX Solar Exposure Under Wavelength Filters (1 wt%).

PRELIMINARY PRODUCTS ANALYSIS OF THE HMX AND RDX PHOTODECOMPOSITION IN KBr

FTIR spectra of the final photolysis products of HMX and RDX in KBr and the dichloromethane (DCM) extract of completely photolyzed HMX are shown in Figure 19. Preliminary FTIR analysis of the solid-phase products, after complete disappearance of the nitramine, show the presence of a nitrate salt (KNO_3) and an alkyl formamide or mixture of formamides (bottom spectrum in Figure 19).

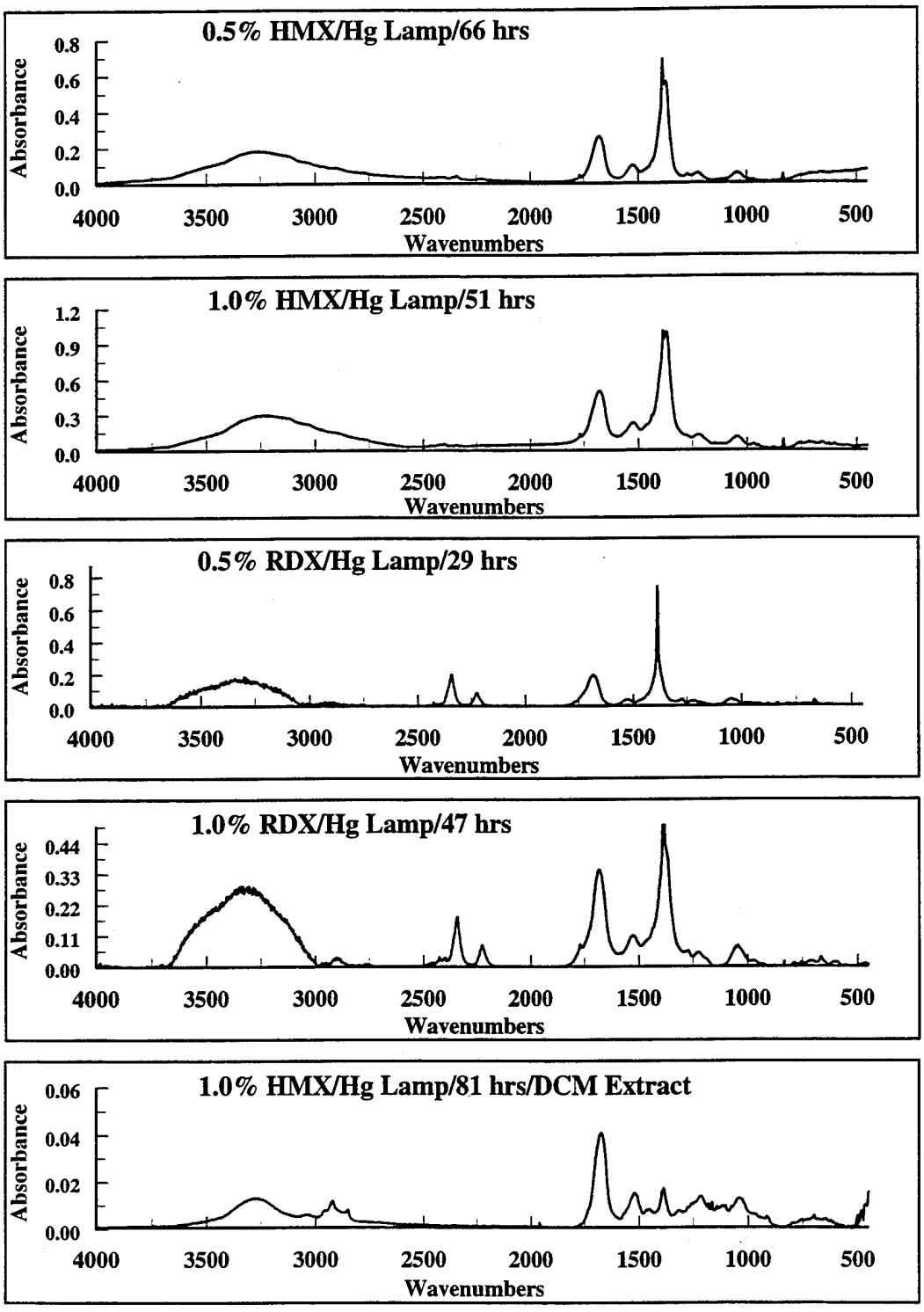

FIGURE 19. FTIR Spectra of RDX and HMX Photolysis Products.

CONCLUSIONS AND RECOMMENDATIONS

RDX and HMX photodecompose in the solid state (dispersed in KBr) at a reasonable rate under both medium-pressure Hg lamp or sun irradiation. The photolysis rate for RDX is faster than for HMX at high concentrations (>2 wt%) and about the same for concentrations below 2 wt%. Both RDX and HMX, dispersed in KBr, photodecompose at an exponential rate that depends upon concentration, path length, wavelength of light, and intensity of light. However, preliminary data show that the rate is also particle-size dependent. Preliminary photolysis products are KNO_3 and alkyl formamides.

Further work is required to determine the photolysis rate in non-dispersed systems, such as neat nitramine and nitramine in sand and soil. The influence of nitramine particle size on the photolysis rate must be determined to calculate actual solar efficiencies. More detailed analysis of the photolysis products and mechanism is required. Finally, a field demonstration of the photodecomposition of RDX and HMX must be conducted to further validate our experimental model.

REFERENCES

1. K. Suryanarayanan and S. Bulusu. "Photolysis of Solid Dimethylnitramine. Nitrogen-15 Study and Evidence for Nitrosamide Rearrangement" *Journal of Physical Chemistry,* Vol. 76, No. 4, pp. 496-500, 1972.

2. N. J. Pitts, Jr., D. Grosjean, K. Van Cauwenberghe, P. J. Schmid, P. J.; D. R. Fitz. "Photooxidation of Aliphatic Amines Under Simulated Atmospheric Conditions: Formation of Nitrosamines, Nitramines, Amides, and Photochemical Oxidant," *Environmental Science and Technology,* Vol. 12, No. 8. pp. 946-954, August 1978.

3. Y. L. Chow, H. Richard, R. W. Snyder, and R. W. Lockhart. "Generation of Aminyl and Aminium Radicals by Photolysis of N-Nitrodialkylamines in Solution," *Canadian Journal of Chemistry,* Vol. 57, p. 2936, 1979.

4. J. Stals, A. S. Buchanan, C. G. Barraclough. "Chemistry of Aliphatic Unconjugated Nitramines," *Transactions Faraday Society*, 67, 1749, (1971). Stals, J., *ibid.*, 67, 1768 (1971). Stals, J., Buchanan, A. S., Barraclough, C. G., *ibid.*, 67, 1756 (1971). Stals, J., *ibid.*, 67, 1739 (1971).

5. Naval Surface Weapons Center. *Photolysis of RDX in Aqueous Solution, with and without Ozone,* by D. J. Glover, J. C. Hoffsommer. NSWC, White Oak Laboratories, Feb 1979. (NSWC TR 78-178, publication UNCLASSIFIED.)

INITIAL DISTRIBUTION

1 Naval Air Systems Command, Arlington (AIR-8.0Y, H. Varmall)
1 Chief of Naval Operations, OP-987
4 Chief of Naval Research, Arlington
    ONR-333
        J. Goldwasser (1)
        R. Miller (1)
    ONR-351, D. Siegel (1)
1 Marine Corps Combat Development Command, Landing Force Development Center, Quantico
  (Technical Library)
6 Naval Sea Systems Command, Arlington
    SEA-06B (1)
    SEA-06U (1)
    SEA-62 (1)
    SEA-63 (1)
    SEA-662 (1)
    SEA-666 (1)
1 Space and Naval Warfare Systems Command, Arlington (SPAWAR-05)
1 Naval Explosive Ordnance Disposal Technology Center, Indian Head (Technical Library)
1 Naval Postgraduate School, Monterey (Technical Library)
1 Naval Research Laboratory (Technical Library)
1 Naval Surface Warfare Center, Carderock Division, Bethesda (Technical Library)
1 Naval Surface Warfare Center Division, Crane (Technical Library)
7 Naval Surface Warfare Center, Indian Head Division, Indian Head
    Code 90 (1)
    Code 910, N. Johnson (1)
    Code 9110, A. Stern (1)
    Code 9110M, W. Koppes (1)
    Code 9410C, C. Gotzmer (1)
    Code 9410D, W. Lawrence (1)
    Technical Library (1)
1 Naval Undersea Warfare Center Division, Newport (Technical Library)
1 Office of Naval Intelligence, National Maritime Intelligence Center (Technical Library)
1 Army Missile Command, Huntsville (AMSMI-RD-PR-R, L. Asaoka)
3 Army Armament Research, Development and Engineering Center, Dover
    SMCAR-AEE
        J. Lannon (1)
        N. Slagg (1)
    Technical Library (1)
5 Army Ballistic Research Laboratories, Aberdeen Proving Ground
    AMSRL-WT-PC, J. Heimerl (1)
    AMSRL-WT-WG, P. Kaste (1)
    DRDAR-BLP (1)
    SLCRB-TB-E (1)
    Technical Library (1)
1 Army Research Laboratory, Adelphi (Technical Library)
1 Army Research Office, Durham (Chemical and Biological Sciences Division)
1 Air Force Academy, USAFA Academy (FJSRL/MC, J. Wilkes)

3 Air Force Armament Division, Eglin Air Force Base
AFTL/MNE (1)
AFTL/MNW (1)
Technical Library (1)
1 Air Force Office of Scientific Research, Bolling Air Force Base (T. Matusko)
1 Air Force Phillips Laboratory, Edwards Air Force Base (OLAC PL/MKPL, C. Merrill)
2 Air Force Wright Laboratories, Dynamics Directorate, Wright-Patterson Air Force Base
WL/MNME
T. Floyd (1)
R. McKenney (1)
1 Advanced Research Project Agency, Arlington (Technical Library)
1 Defense Nuclear Agency, Alexandria (Technical Library)
1 Defense Research and Engineering (Technical Library)
2 Defense Technical Information Center, Alexandria
1 Department of Defense Explosives Safety Board, Alexandria (DDESB-KT)
1 Office Director Defense Research and Engineering (USD(A)DDRE (R/AT/ET), Staff Specialist for Weapons Technology, R. Menz)
3 Lawrence Livermore National Laboratory, Livermore, CA
R. Simpson (1)
W. Tao (1)
Technical Library (1)
2 Los Alamos National Laboratory, Los Alamos, NM
M. Hiskey (1)
Technical Library (1)
1 Sandia National Laboratory, Albuquerque, NM (Technical Library)
1 Aerojet General Corporation, Propulsion Facility, Sacramento, CA (R. Rindone)
1 Batelle Memorial Laboratory, Columbus, OH (Technical Library)
1 CNA Corporation, Alexandria, VA (Technical Library)
1 Fluorochem, Incorporated, Azusa, CA (K. Baum)
1 Institute for Defense Analyses, Alexandria, VA (Technical Library)
1 SRI International, Menlo Park, CA (R. Schmitt)
1 The Johns Hopkins University, Chemical Propulsion Information Agency, Columbia, MD
2 Thiokol Corporation, Utah Operations, Brigham City, UT
T. Highsmith (1)
B. Wardle (1)